

# Characteristics and impact of *Taq* enzyme adsorption on surfaces in microfluidic devices

A. Ranjit Prakash · Matthias Amrein ·  
Karan V. I. S. Kaler

Received: 27 February 2007 / Accepted: 6 April 2007 / Published online: 2 June 2007  
© Springer-Verlag 2007

**Abstract** We investigated the adsorption of *Taq* enzyme, using sessile droplets, on different microfluidic materials. In *propagating adsorption materials*, the contact angle (CA) of a sessile *Taq* droplet continually recedes and collapses due to adsorption. Contrastingly, in *contained adsorption materials* it exhibits an initial reduced CA due to an instantaneous adsorption, however remains time-invariant. Spectrophotometer analysis on SU8, a *propagating adsorption material*, reveals a gradual loss of *Taq* from the droplet onto the surface during droplet collapsing, as opposed to a rapid saturated adsorption in Teflon, a *contained adsorption material*. AFM micrographs of the adsorbed surfaces suggest a network-like structure in SU8 and distinctly different pillar-like structures in Teflon. With this understanding, we have successfully applied a SU8-Teflon coating to impart a time-invariant contact angle with minimal loss of *Taq* in surface microfluidic devices.

**Keywords** Adsorption · *Taq* · PCR · Chip · Protein

## 1 Introduction

Droplet based surface microfluidics (S $\mu$ F), utilizing dielectrophoresis (Ahmed and Jones 2006; Gunji and Washizu 2005) or electrowetting (Paik et al. 2003; Yi and Kim 2006) for actuation and subsequent manipulation of liquid and droplets, is emerging as a promising and new alternative approach to conventional closed channel microfluidics. A simple S $\mu$ F device for liquid actuation (i.e., drawing of liquid from a parent droplet to form satellite picoliter droplets) as shown in Fig. 1 is constructed with a pair of planar microelectrodes patterned on an insulating substrate (e.g., glass or Si) which is then coated with a thin dielectric layer. The dielectric layer should serve two critical functions (Yoon and Garrell 2003) for successful liquid actuation—(1) as an insulator preventing electrolysis and (2) impart the necessary contact angle (i.e., surface tension) at the droplet–surface interface, ideally to induce a sessile droplet contact angle (CA) over 50°. While a number of different materials, either hydrophilic or hydrophobic, may be successfully applied as a dielectric coating for liquid actuation of low ionic strength water droplets, we find that they fail to satisfy the necessary CA requirements when the droplet is comprised of protein suspension.

This experimental work focuses specifically on the characteristics of protein adsorption influencing the CA of a droplet containing the *Thermus aquaticus* (*Taq*) (Kim et al. 1995) DNA polymerase enzyme on various materials relevant to microfluidics. *Taq* polymerase enzyme, a model globular protein (Haynes and Norde 1995), was chosen for this study as it is a critical component in the popular polymerase chain reaction (PCR) DNA amplification method, widely adopted in microfluidic genetic analysis (Hong and Quake 2003; Lagally and Mathies

---

A. R. Prakash (✉) · K. V. I. S. Kaler  
Biosystems Research and Applications Group,  
Department of Electrical and Computer Engineering,  
Schulich School of Engineering, University of Calgary,  
2500 University Drive NW, Calgary, Canada T2N 1N4  
e-mail: aprakash@ucalgary.ca

K. V. I. S. Kaler  
e-mail: kaler@ucalgary.ca

M. Amrein  
Faculty of Medicine, University of Calgary,  
2500 University Drive NW, Calgary, Canada T2N 1N4

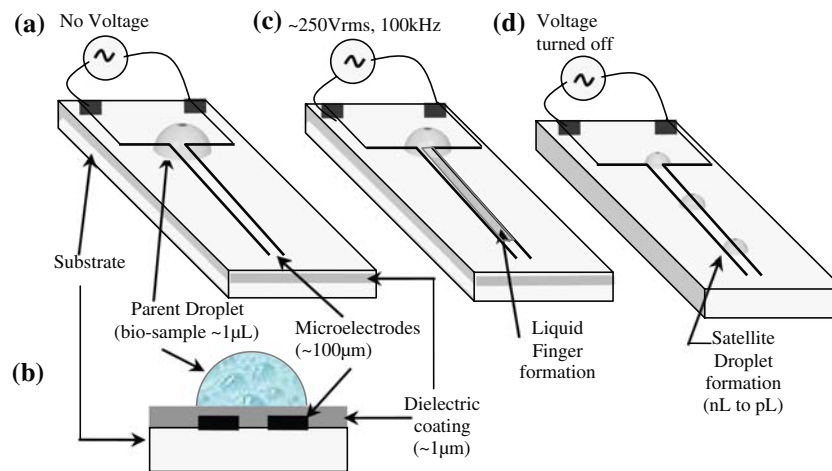


**Fig. 1** **a** A simple surface microfluidic (S $\mu$ F) structure constructed by an insulating substrate with microelectrode patterns coated with a thin dielectric layer. **b** Cross-sectional view showing a parent droplet placed between the electrodes and atop the dielectric coating. **c** When

a voltage is applied to the electrodes, a liquid finger projects from the parent droplet, and **d** satellite droplets are formed once the voltage is turned off. Such S $\mu$ F structures can be utilized to realize valveless microfluidic devices for lab-on-a-chip applications

2004; Prakash and Kaler 2006). Moreover, it has been proven (Erill et al. 2003) that *Taq* adsorption drastically reduces the yield of PCR, invariably to the extent of unsuccessful DNA amplification. Haynes and Norde (1995) have pointed-out that ironically our knowledge of structural rearrangements, driving force(s) and mechanism of protein adsorption is extremely limited, often with many presumptions. Thus, a clear and satisfactory understanding of protein adsorption in materials is pivotal to the successful development and implementation of genetics and proteomic analysis in microfluidic applications, where the yield and success of an assay is often hindered by undesired protein/enzyme adsorption particularly impacted by the miniaturized fluidic environment harnessed in microfluidics (Huber et al. 2003).

Recent studies (Koutsopoulos et al. 2004; Sweryda-Krawiec et al. 2004) have suggested a new interpretation for protein adsorption in which adsorption occurs in either a single or two-steps, in hydrophilic and hydrophobic materials, respectively. However, in this study we noted that for the *Taq* enzyme even a superhydrophobic material (i.e., CA of water  $>150^\circ$ ) can exhibit adsorption behavior similar to a hydrophilic material (i.e., CA  $<60^\circ$ ). Hence for assays involving *Taq* categorizing materials according to their wettability property (i.e., either hydrophilic or hydrophobic) influencing adsorption appears to be inadequate. Therefore in this work we have categorized materials based on their *Taq* adsorption behavior as described below.

In the first category, termed here as *propagating adsorption* materials, a sessile droplet containing the *Taq* enzyme has a tendency to adsorb laterally in a network-like manner onto the surface and continually seek and adsorb

onto virgin surfaces along the periphery of the droplet. This intrinsic adsorption property causes the droplet to collapse with a gradually receding CA, wherein the droplet spreads into a thin film (i.e., the CA is time dependent up to and even after an observed 600 s time period), and a progressive loss of *Taq* from the droplet is noted. The CA in these *propagating adsorption* materials recedes well below  $30^\circ$  making it highly unsuitable for reliable droplet actuation in S $\mu$ F applications demanding a much higher and stable CA, as stated earlier. Contrastingly, in another category of material, termed *contained adsorption* materials, adsorption is almost instantaneous causing an initial reduction in contact angle (i.e., the CA is static or time invariant after 600 s). Importantly, the CA in these materials remains stable, typically CA  $>40^\circ$ , ideally suited for droplet actuation in S $\mu$ F applications. Furthermore in these *contained adsorption* materials, the loss of *Taq* from the droplet saturates immediately after the initial instantaneous adsorption and no further appreciable loss of *Taq* is observed.

Prior *Taq* adsorption studies concluded that this enzyme extensively adsorbs onto surfaces in microfluidic device and adversely affects *Taq* based assays, however, only investigated silicon and glass materials influencing adsorption and speculated the quantity of *Taq* adsorption onto these two surfaces (Erill et al. 2003; Wang et al. 2006). Another adsorption study by Yoon et al. (2003) for electrowetting microfluidic application examined the adsorption of the protein BSA and enzyme lysozyme on a Teflon surface. Their investigation definitively suggested that adsorption of BSA and lysozyme either under passive conditions (i.e., without the influence of an external driving force) or active conditions (i.e., under the influence of an

electric field) occurs onto Teflon causing a reduction in CA of a sessile droplet.

Herein, 13 different materials commonly used in microfluidic devices (including Teflon) are investigated for their *Taq* adsorption behavior and characterized into one of the two classes defined earlier, i.e., *propagating adsorption* or *contained adsorption* material (as defined earlier), by employing the following analysis methods (a) contact angle analysis to observe the change in the CA of a droplet (i.e., change in droplet surface tension), (b) droplet based spectrophotometer analysis to quantify the enzyme adsorbed onto a surface, and (c) atomic force microscope (AFM) to visualize the adsorbed enzyme on a surface.

## 2 Materials and experimental observations

### 2.1 Materials and methods

Table 1 lists 13 different materials (including manufacturer/supplier information) commonly used in microfluidics that were investigated for their *Taq* adsorption behavior. For those materials that were obtained in liquid form, the materials were spin coated (model: WS-400A, Laurell Tech Corporation, USA) on a 2 in. × 4 in. glass slide (Corning Incorporated, USA). The thicknesses of the coatings were measured using a surface profilometer (AlphaStep, Tehcor Inc, USA) and were as follows. These spin coated materials include: SU8 2000.5 (thickness 0.5 μm),

PMMA (1 μm), PDMS (200 μm), Teflon® (1 μm), Mincor® (~1 μm), trimethylchlorosilane™ (<0.2 μm) and HPR504 (~1.1 μm). All other materials were obtained as planar sheets and used as-is; these include: poly(vinylidene chloride), polyethylene glycol, polyethylene and ParaFilm® wax. All materials were handled in a class 100 clean-room environment thereby avoiding surface contamination impacting adsorption.

The *Taq* polymerase enzyme was obtained from three independent suppliers [Invitrogen, USA, (Lot no. 1381637 and 1362544); Applied Biosystems, USA, (Part no. G0581); Fermentas, Canada, (Lot no. 4912)] and was used in identical experiments to confirm the obtained data. The *Taq* enzyme consists of a single polypeptide with an approximate molecular weight of 94 kDa and an elongation of 130 Å in its crystal form. For all of the below analysis, data from a *Taq* enzyme concentration of about 0.30 mg/mL is presented in the following sections. The contamination-free water used for dilution was either deionized water (resistivity 18.5 MΩ-cm) or biological grade water (no DNAs or RNAs detected, Fluka Biochemika, Switzerland).

For the contact angle measurements, the sample was placed on an ice bath, while for the spectrophotometric and AFM measurements the sample was kept in an artificially humidified enclosure (i.e., an ice filled Styrofoam box). The temperature of the surface/enclosure was noted to be between 2 and 6°C, and the relative humidity in the enclosure was about 85%. As a test, we also periodically

**Table 1** Materials commonly used in microfluidic devices investigated here for their *Taq* adsorption behavior using contact angle measurement

Material	Supplier	Contact angle (CA) of sessile droplet			Implied material classification <sup>a</sup>
		DI-H <sub>2</sub> O (time invariant)	<i>Taq</i> (enzyme)		
			<i>t</i> = 5 s	<i>t</i> = 600 s	
Glass	Corning, USA	25°	14°	<8°	Propagating adsorption
Polyethylene glycol (PEG)	J.T. Bakar, USA	35°	25°	<10°	Propagating adsorption
Polymethyl methacrylate (PMMA)	MicroChem, USA	60°	45°	<10°	Propagating adsorption
Poly(vinylidene chloride) (PVDC)	S.C. Johnson, Canada	95°	45°	<20°	Propagating adsorption
Trimethylchlorosilane (SafetyCoat™)	J.T. Baker, USA	95°	52°	<30°	Propagating adsorption
Polyamide	DuPont, USA	55°	55°	<8°	Propagating adsorption
HPR 504	Shiply, USA	60°	58°	<10°	Propagating adsorption
SU8 (2000.5)	MicroChem, USA	60°	60°	<10°	Propagating adsorption
Polyethylene film (PE)	Glad Metric, Canada	65°	60°	<10°	Propagating adsorption
Mincor® S 300	BASF, Germany	165°	115°	<10°	Propagating adsorption
Teflon® AF (polytetrafluoroethylene)	DuPont, USA	110°	60°	58°	Contained adsorption
ParaFilm® Wax film	Ameri. Natl. Can™, USA	115°	46°	43°	Contained adsorption
Poly dimethylsiloxane (PDMS)	Dow Corning, USA	90°	75°	40°	Contained adsorption

<sup>a</sup> Materials on which the contact angle recedes (<30° after 600 s and continues to recede) due to *Taq* (enzyme) adsorption are classified as “*propagating adsorption*” materials, while those with static droplet contact angle (>40° after 600 s and remains time-invariant) are classified “*contained adsorption*” materials. [CA error ±2°]

quantified (Prakash et al. 2006) the volume of droplets ranging from 2 to 10  $\mu\text{L}$  in such an environment for 15 min (well above the time span of our intended adsorption measurements) to verify minimized evaporation losses and noted no appreciable change in volume within a 5% measurement error.

## 2.2 Contact angle measurements

The adsorption of proteins and enzymes is often studied using time-dependent contact angle change, as it facilitates easy visual observation of adsorption impact on a sessile droplet (Orasanu-Gourlay and Bradley 2006; Pancera and Petri 2002; Sweryda-Krawiec et al. 2004; Yoon and Garrell 2003). Moreover as emphasized earlier, CA is a critical parameter (Yoon and Garrell 2003) in S $\mu$ F applications and hence we employed CA analysis for *Taq* adsorption studies on differing surfaces.

The influence of *Taq* adsorption on contact angle for each of the above materials (Table 1) was studied using an automated contact angle analyzer (First Ten Angstroms Instrument, USA). CA measurements were obtained using an automated method similar to that described elsewhere (Cheng et al. 1990). All CA data presented here are the mean of a minimum of three independent measurements. The standard deviation was typically below 4° and the measurement error was  $\pm 2^\circ$ .

For all materials a comparison is drawn between the surface wettability of water [i.e., CA of a de-ionized water (DI-H<sub>2</sub>O) droplet] to a water droplet (or a PCR sample) containing the *Taq*. We observed that while the CA of water droplets on all of these materials was static with no appreciable change over time (within  $\pm 2^\circ$  averaged error), the same is not the case when the droplet contains the *Taq* enzyme. As summarized in Table 1, if a droplet contained *Taq*, one of the following two behaviors was observed. Due to *Taq* adsorption, either the droplet starts to collapse in which case it is categorized as a *propagating adsorption* material, or there is an instantaneous reduction in the CA but no collapsing of the droplet (i.e., static CA) and hence categorized as *contained adsorption* material (note: a detailed definition with criteria for categorization stated earlier). Our finding suggests that *Taq* has a high adsorption affinity to most surfaces (either *propagating* or *contained adsorption* material) and causes a change in CA much more rapidly than most other proteins and enzymes on similar surfaces discussed in literature (Sweryda-Krawiec et al. 2004; Yoon and Garrell 2003).

For a better understanding of the two distinct droplet behaviours, a detailed analysis is provided in Fig. 2 for SU8 and Mincor<sup>®</sup> (*propagating adsorption* materials), compared with Teflon<sup>®</sup> and Wax (*contained adsorption* materials). Presented in Fig. 2 is a CA analysis as a func-

tion of time for both water and *Taq* droplets in these materials. In Fig. 2a–d, *propagating adsorption* materials SU8 (a hydrophilic material with water CA 60°) and Mincor<sup>®</sup> (a superhydrophobic material with water CA 165°), show a receding CA (Gu and Li 1998) due to *Taq* adsorption and within 10 min the CA reduces to  $<10^\circ$ . This passive adsorption causing receding CA is irreversible, unlike an externally induced CA change, example using electric fields (Lam et al. 2001; Yoon and Garrell 2003).

As seen in Fig. 2b, d, the rate of change in CA exhibits a step-wise reduction, especially in the first few minutes, and appears to be similar to a “adsorption-clicks” mechanism of bovine lipid extract surfactant that decreases the surface tension (i.e., CA) as described by Lu et al. (2003). It is worth noting that it is not uncommon for proteins and surfactants to exhibit identical adsorption characteristics influencing CA change (Beverung et al. 1999).

In contrast, *contained adsorption* materials in Fig. 2e–h, namely Teflon (a hydrophobic material with water CA 110°) and Parafilm wax (a hydrophobic material with water CA 115°), a static CA is observed (i.e., no change in CA over time), although due to *Taq* adsorption there is an almost instantaneous reduction in CA by about 50% (i.e., 60° in Teflon and 45° in Parafilm wax) compared to the CA of a pure water droplet. This impact of adsorption on CA is consistent with that observed in literature. For example, an earlier study (Yoon and Garrell 2003) of the proteins BSA and enzyme lysozyme on Teflon showed a ~20% reduction in CA due to adsorption, while for the *Taq* on the same Teflon surface we observe more than double that change occurring more rapidly. In literature (Haynes and Norde 1995; Koutsopoulos et al. 2004), it has been suggested that irreversible adsorption of proteins lead to conformational restructuring and/or extensive spreading of the protein onto a surface. This perhaps explains the herein observed change in CA in differing materials and the reduced PCR yield (Erill et al. 2003; Wang et al. 2006) in microfluidic devices due to *Taq* adsorption.

Srinivasan et al. (2004) have suggested (without characterized evidence) that for low concentration protein suspensions, a possible thin film of oil between the protein droplet and the surface may minimize adsorption. While their claim lacked evidential support, to eliminate any suspicion on the influence of such a possible thin oil film interface impacting CA/adsorption, we replicated the above CA experiments under (mineral and silicone) oil (i.e., emulsion-like environment, wherein the droplet containing water/*Taq* is placed on the surface covered with oil). Since the density of water ( $\rho = 0.98 \text{ g/cm}^3$ ) is greater than oil ( $\rho = 0.93 \text{ g/cm}^3$ ) (Tian et al. 2001), the droplet (containing the *Taq*) quickly sinks to the surface. In this scenario as well, we noted identical droplet collapsing effect in *propagating adsorption* materials and a non-collapsing (with an

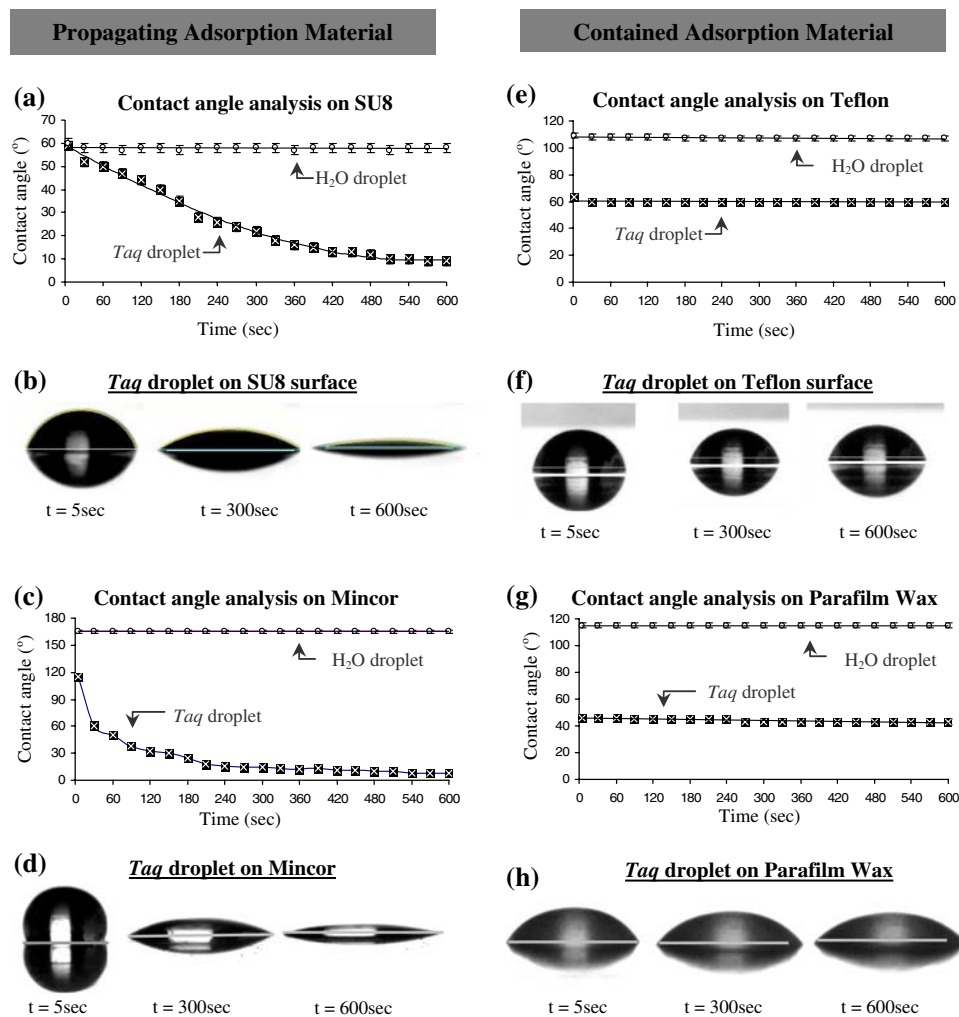


**Fig. 2** Detailed contact angle (CA) analysis of propagating adsorption materials (SU8 and Mincor) and contained adsorption materials (Teflon and Parafilm Wax). The CA measurement for sessile droplets images both the droplet and a reflection of the droplet as seen in the above images. The CA is measured as an average of steepest exterior tangent of the droplet and the reflected image. **a, b** CA analysis on SU8 surface. In 10 min, for a *Taq* droplet the CA recedes gradually from ~60° to 8°, while for DI-H<sub>2</sub>O it remains unchanged at ~60°. **c, d** CA analysis on Mincor surface. Here too the CA recedes, however,

more rapidly from 185° to 8° in 10 min, while the CA of DI-H<sub>2</sub>O remains unchanged at 165°. Note that the CA is incapable of receding beyond 8° due to liquid surface tension effects and furthermore the inability of the analyzer to resolve lower CAs. **e, f** CA analysis on Teflon surface, where a *Taq* droplet has an instantaneous reduction in CA, compared to DI-H<sub>2</sub>O, however, remains unchanged over time (i.e., time invariant or static CA) at 58°; **g, h** a similar effect to Teflon is also observed in Parafilm wax with static CA for *Taq* droplets at 43°

instantaneous reduction in CA) effect in *contained* adsorption materials. This perhaps suggests that at biologically relevant *Taq* concentrations, the thin oil film, if at all present at the interface, may well be squeezed out from the droplet–surface interface because proteins can lower the liquid–oil interfacial tension (Beverung et al. 1999), as rightly speculated by Srinivasan et al. (2004).

### 2.3 Spectrophotometer analysis

The purpose of the spectrophotometric studies was to further investigate the adsorption on SU8 (a *propagating*

*adsorption* material) and Teflon (a *contained adsorption* material) coated surfaces, since more recently these two materials are popularly used in emerging droplet based S<sub>μ</sub>F devices (Jenke et al. 2007; Paik et al. 2003; Sato et al. 2006; Wang et al. 2007; Xu et al. 2006; Yi and Kim 2006; Yoon and Garrell 2003). The adsorption in these materials was studied by monitoring (ND-1000, NanoDrop, USA) the amount of *Taq* enzyme adsorbed onto the surfaces over a comparable time scale as the earlier CA measurements. Here 2 μl droplets, with a measured initial *Taq* concentration, were placed on the surface for varying time periods (60–300 s), before it was retrieved (Prakash et al. 2006)

from the surface and analyzed to determine the remaining concentration of the *Taq* in the droplet. The inverse of such measurements provides the implied adsorption on a surface, the findings of which are shown in Fig. 3. It is readily apparent that the initial *Taq* adsorption, both in SU8 and Teflon surfaces, is very rapid (i.e., <60 s), similar in characteristic to that reported by Story et al. (1991) for other enzymes. However, beyond this short time period adsorption activity, adsorption in SU8 and Teflon show dissimilar behavior as explained below.

In SU8, the concentration of *Taq* in the droplet steeply dropped from the initial 0.29 to 0.20 mg/mL during the first 60 s. Beyond this time, the enzyme loss in the droplet occurred more gradually and within 300 s the concentration in the droplet fell to 0.14 mg/mL. This two-phase loss of enzyme concentration from the droplet implies a ~50% adsorption of the *Taq* onto the SU8 surface. As indicated in Fig. 3 this phenomenon is seen as a gradual increase in the *Taq* adsorbed onto SU8 reaching an adsorption value of 0.15 mg/mL in 300 s. It has been postulated (Beverung et al. 1999) that such changes in the rate of adsorption is a consequence of an initial interfacial conformational change and a subsequent ratio of protein-to-surface interaction that influences phased adsorption. Although it is alluring to attribute the time dependent continual *Taq* adsorption on SU8 to a ~200% change in surface area as a result of droplet spreading, this is clearly not the only contributing factor, as suggested subsequently by the AFM investigations of the SU8 and Teflon surfaces.

Contrastingly, in Teflon while the *Taq* concentration initially dropped from 0.29 to 0.22 mg/mL, a 25% loss, unlike SU8 no further loss was observed in the remainder of the 300 s experimental time frame. As seen in Fig. 3, adsorption onto the Teflon surface reaches a saturated *Taq* adsorption concentration of 0.07 mg/mL. Although the first adsorption data-point was obtained after 60 s due to mea-

surement constraints, this *Taq* adsorption in Teflon is believed to be an almost instantaneous adsorption, as implied from the earlier CA measurements wherein the droplet containing *Taq* shows an instantaneous reduction in CA by nearly half compared to pure water.

Clearly, unlike Teflon, which exhibits a time invariant adsorption, the SU8 coated surface continues to adsorb *Taq* unabated, over the 300 s time period investigated. [Note: due to the constraints with our spectrophotometric measurements, adsorption data could not be obtained if the CA receded below 20° (i.e., >300 s for *Taq* droplets on SU8). Hence all spectroscopic measurements were made within 300 s].

#### 2.4 AFM scanning

AFM measurements (NanoWizard, JPK Instruments, Germany) reported here principally focused on high-resolution nanoscale examination of the SU8 and Teflon surfaces, after *Taq* adsorption. The AFM scans were performed in tapping mode with a silicon tip (Tap200A1, mechanical resonance frequency: 300 kHz, force constant: 40 N/m, Budget Sensors, Bulgaria). For comparison purposes AFM micrographs of an example area of both bare SU8 and Teflon, and *Taq* adsorbed SU8 and Teflon surfaces are shown in Fig. 4a–d. The surface morphologies of the bare SU8 (Fig. 4a) and Teflon (Fig. 4c) appear to be identical and are considered smooth surfaces with a maximum surface roughness of about ~1.5 nm.

Upon adsorption on the two surfaces, it is readily evident that the *propagating adsorption* material SU8 shows surface landscape with massive and unordered deposition of *Taq*, ranging up to about 700 nm in height (Fig. 4b). There appears to be islands of *Taq* aggregation in a network like fashion, similar to that observed for other proteins in literature (Orasanu-Gourlay and Bradley 2006). Contrastingly, Teflon surface exhibits only a scarce adsorption of *Taq* and furthermore, the adsorbed species form pre-dominantly high aspect-ratio 200 nm pillar-like structures on the surface (Fig. 4d), easily distinguishable from a SU8 adsorbed surface.

The amount of adsorbed *Taq* in either SU8 or Teflon surface has been quantified by the earlier spectrophotometer analysis with good confidence. In addition, we performed a semi-qualitative comparison of the *Taq* adsorbed SU8 (Fig. 4b) and Teflon (Fig. 4d) surfaces from the AFM images. AFM image analysis to produce adsorption estimation was performed using the following techniques: (a) image contrast-threshold increment to distinguish background from *Taq* adsorbed area, (b) background subtraction method to remove portions of un-adsorbed area, and (c) pixel based histogram analysis to quantify the height of the adsorbed structures. From the SU8 and Teflon adsorbed

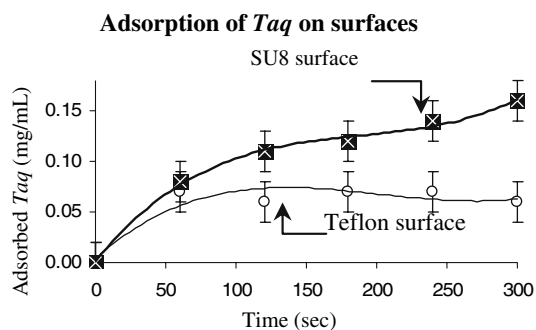


**Fig. 3** Spectrophotometer analysis quantifying *Taq* adsorption on surfaces. In both SU8 and Teflon, categorized as propagating and contained adsorption materials, respectively, an initial rapid adsorption is observed. This is followed by a gradually increasing adsorption of *Taq* in SU8 (0.15 mg/mL in 5 min). In Teflon however the initial adsorbed amount (0.07 mg/mL) is the saturated value

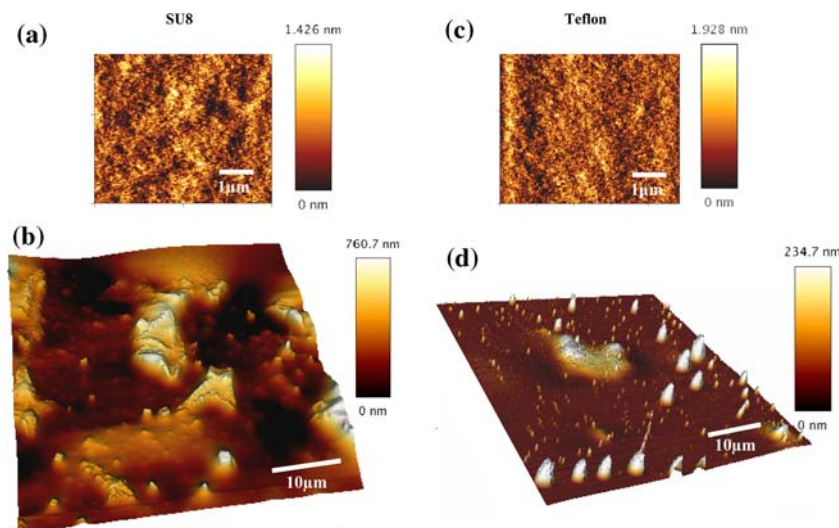


**Fig. 4** AFM scans of **a** SU8 surface, a *propagating adsorption* material, and **c** Teflon surface, a *contained adsorption* material, showing smooth surface topologies. **b** a SU8 *Taq* adsorbed surface appears as a aggregation and network of the *Taq* in a propagating manner. This perhaps explains the droplet collapsing phenomena where the droplet CA recedes until it spreads into a thin film.

processed images, we estimate  $\sim 75\%$  more adsorption in SU8, as compared to Teflon. However, this appears inconsistent from the earlier (actual) *Taq* concentration measurements using the spectrophotometer, which indicated only a 50% increased adsorption in SU8. We reason that the AFM image analysis for adsorption quantification may be inaccurate for the following reasons, (1) the scanned area ( $2,500 \mu\text{m}^2$ ) is only a fraction of the total droplet–surface contact area, (2) the density of the adsorbed structures is unknown and assumed to be homogenous, and (3) the adsorbed surface appears random and unordered, as evident from the AFM micrographs; however, the AFM adsorption estimations assumes a adsorption pattern for the entire droplet–surface contact area to be identical to the fractional AFM scanned area. Evidently, for our study the AFM micrographs/images are best suited for nanoscale observations rather than adsorption quantifications.

Nevertheless, it is apparent that the SU8 adsorbed surface landscape is very different, showing massive and unordered adsorption of *Taq* enzyme, compared to pillar structures in Teflon. This suggests that the adsorption on Teflon is significantly different from that on SU8 and furthermore, where in one case SU8 gives rise to large propagating structures causing droplet collapsing, in the case of Teflon, the pillar like structures are non-propagating or contained beneath the non-collapsing droplet area, another feature from which the categorization names were coined. These pillar-like arrangements perhaps contribute to higher CA in adsorbed Teflon surfaces as compared to

Contrastingly, in Teflon **d** the *Taq* adsorption appears scarcely in pillar structures and contained beneath the droplet. Droplet collapsing is not observed in Teflon, however, for droplets containing the *Taq*, a 50% instantaneous reduction in CA is noticed, as compared to pure water, attributed to the *Taq* adsorption

SU8, similar to artificially fabricated pillar structures (McHale et al. 2005) that induce high CA.

## 2.5 PCR assay

Some materials are known to inhibit the PCR (Shoffner et al. 1996). To verify the compatibility of Teflon in  $\text{S}\mu\text{F}$  applications involving *Taq* assays (e.g., PCR), a droplet PCR experiment was performed. A *Taq* polymerase PCR sample was prepared (Prakash et al. 2005) with siRNA vector template with primer sequences, 5'-CTG GGA AAT CAC CAT AAA CGT GAA-3' and 5'-GCT TAC CGT AAC TTG AAA GTA TTT CG-3'. Droplet of the PCR sample (1, 3 and 5  $\mu\text{L}$ ) were then placed on a Teflon coated glass surface and overlaid with oil to prevent evaporation during thermal cycling. Upon completion of 35 thermal cycles (94°C for 30 s and 68°C for 30 s), the samples was retrieved and analyzed by capillary electrophoresis (CE) (Prakash and Kaler 2006). The CE electropherogram of the PCR (3  $\mu\text{L}$ ) confirmed the successful amplification of a 340 bp product as shown in Fig. 5, confirming the non-inhibiting nature of the Teflon surface for PCR assays. Moreover, the yield of the droplet PCR experiments were comparable with conventional tube PCR (data not shown), suggesting minimal adsorption of *Taq* onto Teflon that does not adversely impact the PCR. Furthermore, the yield of the droplet PCR assays on Teflon surface remained consistent, within the detection limits of CE, even with varying reaction droplet volumes (1–5  $\mu\text{L}$ ). This complements our

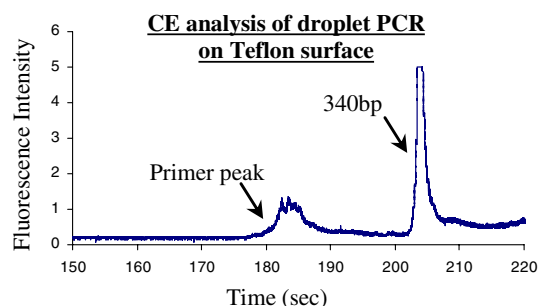


**Fig. 5** Electropherogram of droplet PCR sample on Teflon surface using siRNA vector sample. A weak primer peak is seen at 185 s and strong 340 bp amplification is seen at ~205 s. The length of the resulting product was verified by arrival time of the fluorescence peak. The Teflon surface coating did not inhibit the PCR reaction and is also ideally suited for surface or closed-channel microfluidic devices, as it is a *contained adsorption* material for *Taq* (i.e., relatively less adsorption with time-invariant droplet contact angle)

earlier time invariant CA and adsorption measurements of Teflon surfaces.

### 3 Discussion

Herein, we have combined macroscale observation, such as droplet contact angle and adsorption concentration measurements, with nanoscale AFM data to compare the adsorption of the *Taq* enzyme on “*propagating*” and “*non-propagating* or *contained*” materials utilized in  $\mu\text{F}$  based biochemical applications.

Although we found that the *Taq* has different adsorption rate on different materials/surfaces (inferred from the time-dependent change in CA and spectrophotometer analysis), this is not uncommon for protein/enzyme adsorption. While, to the best of our knowledge, no detailed adsorption study is available for the *Taq*, a number of prior studies using other commonly used proteins such as lysozyme (Assis 2003; Beverung et al. 1999; Haynes et al. 1994; Luk et al. 2000; Norde and Favier 1992; Prime and Whitesides 1993; Story et al. 1991; Yoon and Garrell 2003), creatine phosphokinase (Pancera and Petri 2002), glucose 6-phosphate dehydrogenase (Pancera and Petri 2002), bovine serum albumin (Haynes and Norde 1995; Norde and Favier 1992; Popat and Desai 2004; Sweryda-Krawiec et al. 2004; Yoon and Garrell 2003), immunoglobulin (Vermeer et al. 2001), and many other proteins/enzymes have invariably shown unique adsorption rates on different materials, including some of the materials/surface presented in this work. The differences in rate of adsorptions may be attributed to a number of inter-playing mechanisms commonly postulated in literature including: tendency of protein hydrophobic/hydrophilic chain to either align towards

(or away) from the adsorbing surface (Koutsopoulos et al. 2004; Orasanu-Gourlay and Bradley 2006; Pancera and Petri 2002), surface free-energy (i.e., charge) (Noinville et al. 2002), electrostatic attraction/repulsion (Assis 2003; Haynes et al. 1994; Yoon and Garrell 2003), thermodynamics (Haynes and Norde 1995; Norde and Haynes 1995), unique interfacial tension between the protein and adsorbing surface (Beverung et al. 1999), and relationship between protein penetration and steric hindrance from the structure of the protein and adsorbing material (Luk et al. 2000; Moskovitz and Srebnik 2005; Sofia et al. 1998). It is worth noting that many authors have suggested that the adsorption mechanisms themselves may not be fully understood (Haynes and Norde 1995; Luk et al. 2000; Sweryda-Krawiec et al. 2004; Yeo et al. 2006).

Our study focused on the experimental characterization and impact of *Taq* adsorption onto materials commonly used in microfluidic PCR applications; hence it is beyond the scope of the current study to assertively attribute the *Taq* adsorption to any one of the above mechanisms. However, our data suggest that *Taq* adsorption in *propagating* adsorption materials is uniquely distinct from that occurring in *contained* adsorption materials and this difference may be postulated to be a combination of any (or all) of the above known adsorption mechanism. Furthermore, from literature evidence (Beverung et al. 1999; Haynes and Norde 1995; Koutsopoulos et al. 2004), it may, however, be postulated that the irreversible adsorption phenomena causing conformational restructuring and/or extensive spreading of the protein onto a surface due to interfacial tension best describes our observed droplet CA change behavior. It is also worth noting that, within the limitations of the current *Taq* adsorption study of the 13 different materials, those that fell into the *propagating adsorption* category include hydrophilic, hydrophobic as well-as superhydrophobic surfaces, while those in the *contained adsorption* category include only hydrophobic surfaces.

Nevertheless, our finding suggests that Teflon provides a superior surface coating for  $\mu\text{F}$  applications, one that exhibits minimal adsorption, as compared to other surfaces listed in Table 1. Furthermore, on Teflon the adsorbed species give rise to nanoscale structures which may be responsible for maintaining a larger contact angle (D’Urso et al. 2007), compared to SU8 or even other superhydrophobic materials (e.g., Mincor<sup>®</sup>, see Table 1). Thus for biological applications utilizing open or closed channel microfluidic requiring considerable adsorption preclusion, Teflon is a more versatile, biocompatible (Lehmann et al. 2006) coating for handling complex fluidic samples (e.g. PCR samples). Alternatively, for biofilm applications requiring surface-immobilized proteins benefit from monolayer adsorption and hence *propagating adsorption*



materials listed in Table 1 (including SU8) can be advantageously utilized (Pancera and Petri 2002).

While data presented above were obtained from 0.3 mg/mL, we also noted that *Taq* concentration (i.e., dilution in pure water with no ions) ranging from a minimal concentration as low as 0.1 mg/mL to as high as 1 mg/mL, a range outside the concentration typically used in PCR experiments, yielded identical adsorption behavior as presented earlier. Furthermore, we observed that the dilution of the *Taq* enzyme in a commonly used ionic buffer solution TBE (Tris–Boric Acid–EDTA, OmniPur, USA) at biologically relevant buffer strengths ranging from 0.1 to 10 $\times$ , also exhibited identical droplet behavior. This suggests that the suspension of *Taq* in most biological samples (e.g., PCR solution, pure water, salt buffers) does not affect its strong enzyme–surface interaction and adsorption.

A few studies (Bi et al. 2006; Luk et al. 2000; Popat and Desai 2004; Prime and Whitesides 1993) have found polyethylene glycol (PEG) and its derivatives to have reduced affinity to proteins. We however found PEG to be a *propagating adsorption* material in the case of *Taq* samples, causing a droplet to collapse as indicated in Table 1. This implies that it may not be suitable for  $\mu$ F applications involving *Taq* assays. Moreover, PEG could not be utilized in our  $\mu$ F application because the water CA on PEG is only about 35° (Popat and Desai 2004), well below our minimal  $\sim$ 50° requirement for droplet liquid actuation in  $\mu$ F. In prior work (Kanagasabapathi et al. 2006) we have shown that SU8 dielectric coating, one of the *propagating adsorption* materials investigated here, enables successful liquid actuation, however, exhibits rapid receding CA for droplets containing the *Taq*. On the other hand, Teflon, a *contained adsorption* material, only exhibits an instantaneous adsorption with an induced static CA of  $\sim$ 60° for *Taq* droplets, a CA ideally suited for  $\mu$ F liquid actuation. However, Teflon has very poor adhesion to glass resulting in unreliable coating and also has a lower dielectric strength compared to SU8 ( $K_{\text{Teflon}}:2.1$ ,  $K_{\text{SU8}}:3$ ). Hence, we adopted (Kanagasabapathi et al. 2006) a two-layer coating for  $\mu$ F liquid actuation applications using *Taq* samples—a SU8 underlying coating (0.5  $\mu$ m) to provide the dielectric properties and adhesion strength to an upper Teflon coating ( $\sim$ 0.6  $\mu$ m) which prevents droplet collapsing and provides the necessary *Taq* droplet time-invariant CA of  $\sim$ 60°. This SU8–Teflon composite coating only demanded a  $\sim$ 15% increase in actuation voltage as compared a SU8 only dielectric coating. Furthermore, this composite coating exhibited (Kanagasabapathi et al. 2006) good coating integrity (i.e., no visible wear/tear) even after 2 h of rapid PCR thermal cycling (50°–95°) and a time-invariant *Taq* droplet CA even at this elevated temperature condition.

## 4 Conclusion

In conclusion, herein we have provided a detailed contact angle analysis of sessile droplets that are influenced by *Taq* adsorption on a number of differing materials/surfaces (listed in Table 1), followed by spectrophotometer and AFM analysis of SU8 and Teflon surfaces, as examples of *propagating* and *contained* adsorption materials. We found that in *propagating* adsorption materials (e.g., SU8), *Taq* adsorption occurs continually and within 10 min the droplet completely collapses. Contrastingly, in contained adsorption materials (e.g., Teflon), there is an instantaneous reduction in contact angle ( $\sim$ 50%) due to *Taq* adsorption, however, the contact angle remains time-invariant past the initial change. Spectrophotometric analysis to determine the loss of adsorbed *Taq* complements and supports the contact angle data as it reveals a continual loss of *Taq* in SU8 while adsorption saturation is quickly reached on a Teflon surface. AFM micrographs further confirmed the massively adsorbed *Taq* on SU8 surface and scarcely pillar-like adsorbed structures on Teflon. Undoubtedly, Teflon therefore offers a superior surface coating especially for  $\mu$ F applications involving protein/enzyme assays, with minimal adsorption behavior.

The present study provides a practical application oriented understanding of *Taq* adsorption on materials commonly used in microfluidics. This is hoped to benefit the  $\mu$ F microfluidic community in choosing materials/coating that will best suit an application involving *Taq* assays, particularly the PCR. Efforts are currently in progress for further investigation into each of the materials listed in Table 1 using measurement methods presented here and other techniques (e.g., ellipsometry for adsorbed monolayer observation and MEMS cantilevers for mass quantification). This is hoped to overcome the current measurement limitation and provide a real-time understanding of the adsorption mechanism, particularly in shorter time scales.

**Acknowledgments** We would like to acknowledge the funding, provided by Natural Science and Engineering Research Council (NSERC) of Canada and Western Economic Diversification (WED) Canada in support of work presented.

## References

- Ahmed R, Jones TB (2006) Dispensing picoliter droplets on substrates using dielectrophoresis. *J Electrostat* 64(7–9):543–549
- Assis OBG (2003) Scanning electron microscopy study of protein immobilized on SiO<sub>2</sub> sol–gel surfaces. *Braz J Chem Eng* 20(3):339–342
- Beverung CJ, Radke CJ, Blanch HW (1999) Protein adsorption at the oil/water interface: characterization of adsorption kinetics by

- dynamic interfacial tension measurements. *Biophys Chem* 81(1):59–80
- Bi HY, Meng S, Li Y, Guo K, Chen YP, Kong JL, Yang PY, Zhong W, Liu BH (2006) Deposition of PEG onto PMMA microchannel surface to minimize nonspecific adsorption. *Lab Chip* 6(6):769–775
- Cheng P, Li D, Boruvka L, Rotenberg Y, Neumann AW (1990) Automation of axisymmetric drop shape-analysis for measurement of interfacial-tensions and contact angles. *Colloids Surf* 43(2–4):151–167
- D'Urso B, Simpson JT, Kalyanaraman M (2007) Emergence of superhydrophobic behavior on vertically aligned nanocone arrays. *Appl Phys Lett* 90(4):044102
- Erill I, Campoy S, Erill N, Barbe J, Aguilo J (2003) Biochemical analysis and optimization of inhibition and adsorption phenomena in glass–silicon PCR-chips. *Sens Actuators B Chem* 96(3):685–692
- Gu YG, Li DQ (1998) A model for a liquid drop spreading on a solid surface. *Colloids Surf A Physicochem Eng Asp* 142(2–3):243–256
- Gunji M, Washizu M (2005) Self-propulsion of a water droplet in an electric field. *J Phys D Appl Phys* 38(14):2417–2423
- Haynes CA, Norde W (1995) Structures and stabilities of adsorbed proteins. *J Colloid Interface Sci* 169(2):313–328
- Haynes CA, Sliwinsky E, Norde W (1994) Structural and electrostatic properties of globular-proteins at a polystyrene water interface. *J Colloid Interface Sci* 164(2):394–409
- Hong JW, Quake SR (2003) Integrated nanoliter systems. *Nat Biotechnol* 21(10):1179–1183
- Huber DL, Manginell RP, Samara MA, Kim BI, Bunker BC (2003) Programmed adsorption and release of proteins in a microfluidic device. *Science* 301(5631):352–354
- Jenke MG, Schreiter C, Kim GM, Vogel H, Brugger J (2007) Micropositioning and microscopic observation of individual picoliter-sized containers within SU-8 microchannels. *Microfluidics Nanofluidics* 3(2):189–194
- Kanagasabapathi T, Prakash AR, Kaler VK (2006) Integration of surface microfluidics to closed-channel fluidics to realize a valveless multi-layer genetic analysis chip. Paper presented at the microTAS. Tenth international conference on miniaturized systems for chemistry and life sciences, microTAS Tokyo, Japan 2:1040–1042
- Kim Y, Eom SH, Wang JM, Lee DS, Suh SW, Steitz TA (1995) Crystal-structure of thermus-aquaticus DNA-polymerase. *Nature* 376(6541):612–616
- Koutsopoulos S, van der Oost J, Norde W (2004) Adsorption of an endoglucanase from the hyperthermophilic *Pyrococcus furiosus* on hydrophobic (polystyrene) and hydrophilic (silica) surfaces increases protein heat stability. *Langmuir* 20(15):6401–6406
- Lagally ET, Mathies RA (2004) Integrated genetic analysis microsystems. *J Phys D Appl Phys* 37(23):R245–R261
- Lam CNC, Ko RHY, Yu LMY, Ng A, Li D, Hair ML, Neumann AW (2001) Dynamic cycling contact angle measurements: study of advancing and receding contact angles. *J Colloid Interface Sci* 243(1):208–218
- Lehmann U, Vandevyver C, Parashar VK, Gijs MAM (2006) Droplet-based DNA purification in a magnetic lab-on-a-chip. *Angew Chem Int Ed* 45(19):3062–3067
- Lu JJ, Yu LMY, Cheung WWY, Policova Z, Li D, Hair ML, Neumann AW (2003) The effect of concentration on the bulk adsorption of bovine, lipid extract surfactant. *Colloids Surf B Biointerfaces* 29(2–3):119–130
- Luk YY, Kato M, Mrksich M (2000) Self-assembled monolayers of alkanethiolates presenting mannitol groups are inert to protein adsorption and cell attachment. *Langmuir* 16(24):9604–9608
- McHale G, Aqil S, Shirtcliffe NJ, Newton MI, Erbil HY (2005) Analysis of droplet evaporation on a superhydrophobic surface. *Langmuir* 21(24):11053–11060
- Moskovitz Y, Srebnik S (2005) Mean-field model of immobilized enzymes embedded in a grafted polymer layer. *Biophys J* 89(1):22–31
- Noirville S, Revault M, Baron MH (2002) Conformational changes of enzymes adsorbed at liquid–solid interface: relevance to enzymatic activity. *Biopolymers* 67(4–5):323–326
- Norde W, Favier JP (1992) Structure of adsorbed and desorbed proteins. *Colloids Surf* 64(1):87–93
- Norde W, Haynes CA (1995) Reversibility and the mechanism of protein adsorption. In: *Proteins at interfaces II*, vol 602. American Chemical Society, Washington, pp 26–40
- Orasanu-Gourlay A, Bradley RH (2006) Protein adsorption by basal plane graphite surfaces: molecular images and nano-structured films. *Adsorption Sci Technol* 24(2):117–130
- Paik P, Pamula VK, Pollack MG, Fair RB (2003) Electrowetting-based droplet mixers for microfluidic systems. *Lab Chip* 3(1):28–33
- Pancera SM, Petri DFS (2002) Formation of enzymatic biofilms on polymer films and on silicon wafers. *Mol Cryst Liq Cryst* 374:611–616
- Popat KC, Desai TA (2004) Poly(ethylene glycol) interfaces: an approach for enhanced performance of microfluidic systems. *Biosens Bioelectron* 19(9):1037–1044
- Prakash R, Kaler KVIS (2006) An integrated genetic analysis microfluidic platform with valves and a PCR chip reusability method to avoid contamination. *Microfluidics Nanofluidics* 3(2):177–187
- Prakash AR, Pilarski LM, Backhouse CJ, Kaler KVIS (2005) An integrated and reusable array PCR genetic amplification and CE detection microfluidic chip with incorporated valves. Paper presented at the Ninth International Conference on Miniaturized Systems for Chemistry and Life Sciences, MicroTAS ( $\mu$ TAS), microTAS Boston 1:145–147
- Prakash AR, Adamia S, Sieben V, Pilarski P, Pilarski LM, Backhouse CJ (2006) Small volume PCR in PDMS biochips with integrated fluid control and vapour barrier. *Sens Actuators B Chem* 113(1):398–409
- Prime KL, Whitesides GM (1993) Adsorption of proteins onto surfaces containing end-attached oligo(ethylene oxide)—a model system using self-assembled monolayers. *J Am Chem Soc* 115(23):10714–10721
- Sato H, Matsumura H, Keino S, Shoji S (2006) An all SU-8 microfluidic chip with built-in 3D fine microstructures. *J Micromech Microeng* 16(11):2318–2322
- Shoffner MA, Cheng J, Hvichia GE, Kricka LJ, Wilding P (1996) Chip PCR. I. Surface passivation of microfabricated silicon-glass chips for PCR. *Nucleic Acids Res* 24(2):375–379
- Sofia SJ, Premnath V, Merrill EW (1998) Poly(ethylene oxide) grafted to silicon surfaces: grafting density and protein adsorption. *Macromolecules* 31(15):5059–5070
- Srinivasan V, Pamula VK, Fair RB (2004) An integrated digital microfluidic lab-on-a-chip for clinical diagnostics on human physiological fluids. *Lab Chip* 4(4):310–315
- Story GM, Rauch DS, Brode PF, Marcott C (1991) Enzymes adsorbed onto model surfaces—infrared-analysis. *ACS Symp Ser* 447:225–236
- Sweryda-Krawiec B, Devaraj H, Jacob G, Hickman JJ (2004) A new interpretation of serum albumin surface passivation. *Langmuir* 20(6):2054–2056
- Tian Y, Meng YG, Wen SZ (2001) ER fluid based on zeolite and silicone oil with high strength. *Mater Lett* 50(2–3):120–123

- Vermeer AWP, Giacomelli CE, Norde W (2001) Adsorption of IgG onto hydrophobic teflon. Differences between the F-ab and F-c domains. *Biochim Biophys Acta Gen Subj* 1526(1):61–69
- Wang W, Wang HB, Li ZX, Guo ZY (2006) Silicon inhibition effects on the polymerase chain reaction: a real-time detection approach. *J Biomed Mater Res Part A* 77A(1):28–34
- Wang KL, Jones TB, Raisanen A (2007) Dynamic control of DEP actuation and droplet dispensing. *J Micromech Microeng* 17(1):76–80
- Xu BJ, Lee YK, Jin QH, Zhao JL, Ho CM (2006) Multilayer SU-8 based microdispenser for microarray assay. *Sens Actuators A Phys* 132(2):714–725
- Yeo SH, Choi CR, Jung D, Park HY (2006) Investigation of protein adsorption using plasma treatment for protein chips. *J Korean Phys Soc* 48(6):1325–1328
- Yi UC, Kim CJ (2006) Characterization of electrowetting actuation on addressable single-side coplanar electrodes. *J Micromech Microeng* 16(10):2053–2059
- Yoon JY, Garrell RL (2003) Preventing biomolecular adsorption in electrowetting-based biofluidic chips. *Anal Chem* 75(19):5097–5102